Wave Run-up and Inline Force Around A Truncated Vertical Circular Cylinder with Different Submergence Depths

XIONG Hong, YANG Jianmin, TIAN Xinliang
(State Key Laboratory of Ocean Engineering, Shanghai Jiao Tong University, Shanghai 200030)

Abstract: Cylindrical structures are widely applied in offshore engineering. Interactions between the waves and offshore structures have been one research hotspot in the field of ocean engineering. This paper focuses on the wave run-up and inline force around a truncated vertical circular cylinder. Experimental studies are carried out in the wave flume at Shanghai Jiao Tong University in China. The diameter of the cylinder (D) is 10 cm and five submergence depths (h_s), i.e., h_s=0.5D, 1D, 2D, 3D, 4D, are considered, respectively. For a cylinder, the results clearly show decreases in the non-dimensional magnitudes of the inline force with the decreasing incident-wave steepness or the increasing scatter parameter. But for the cylinder with different submergence depths, there are different relationships between the inline force and submergence depths.

Key words: wave run-up; inline wave force; submerged depths

1 Introduction

With the development and utilization of marine energy and resources, more and more artificial structures are designed and constructed for the ocean resource exploitation. Offshore structures such as wind turbine foundations, drilling pipes and floating vessels are constantly confronted by danger from wave impact. The wave related problems such as wave run-up, motion response and wave loads of the offshore structures at sea are the main concern and research topics in the ocean engineering community.

In recent times, several attempts have been made to analyze the wave run-up and wave loads on the vertical circular cylinder. The investigations are both analytical and experimental. On the analytical side, Morison equation[1] is applied in small scale structures and McCamy-Fuchs solution[2]is applied in large scale structures. Both of them are for computing the first-harmonic force. For the truncated cylinder, Yılmaz and Incecik[3]studied the analytical solution of the diffraction problem of a group of truncated vertical cylinders. On the experimental side, Galvin and Hallermeier[4]firstly made an experiment on a vertical cylinder about wave run-up. Huseby and Grue[5]conducted an experimental investigation of higher-harmonic wave forces on a vertical cylinder.

In this study, physical experiments are conducted for regular waves interacting with the semi-submerged vertical circular cylinder with different submergence depths, a typical configuration for a floating offshore wind turbine foundation.

2 Experimental equipment and set-up

The physical experiments were conducted in the wave basin at Shanghai Jiao Tong University. The wave tank is 20 m long, 1 m wide and 1.2 m deep. It is glass-walled at one side flume and equipped with a permeable arc-slope wave absorbing beach downstream.

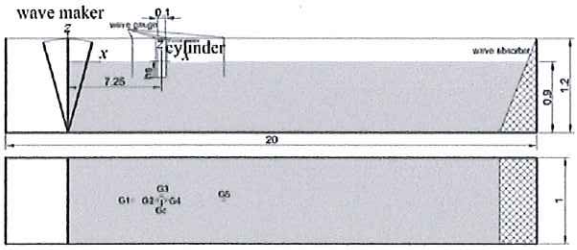

Fig. 1. The general arrangement sketch (unit: m). G1-G5 are the wave gauges, Gc refers to the gauge for wave calibration. The Global Coordinate System is expressed as X, Z, and the Local Coordinate System is expressed as x, z.

Five wave gauges were equipped for the experiments. G1 and G5 are for environmental wave elevations, while G2, G3 and G4 are for the measurement of wave elevations around the cylinder.

Table 1 Particulars of the cylinder (unit: cm)

Particulars	value
Diameter	10.00
Height	29.4/34.4/44.4/54.4/64.4
Submerge depth	5/10/20/30/40

This work was financially supported by Shanghai Yang Fan Program (Grant No. 15YF1406100) and National Natural Science Foundation of China (Grant No. 51239007).

The particulars of cylinder are shown in Table 1. The positions of wave probes are shown in Table 2. The particulars of wave parameters are shown in Table 3.

Table 2 Positions of wave gauges

Gauge	Radial distance from wall /m	Angle from wave direction/(°)	Gauge	Distance from wave paddle/m	Angle from wave direction/(°)
G2	0.004	0	G1	5	0
G3	0.004	90	G5	12	0
G4	0.004	180	Gc	7.25	0

Table 3 Parameters for the incident waves

T /s	*L* /m	*H*/m	*kA*	*kR*	*kd*
0.4	0.25	0.008－0.029	0.1－0.361	1.258	22.637
0.5	0.39	0.006－0.044	0.05－0.361	0.805	14.487
0.6	0.562	0.009－0.065	0.05－0.361	0.559	10.061
0.7	0.765	0.012－0.088	0.05－0.361	0.411	7.392
0.8	0.999	0.016－0.114	0.05－0.361	0.314	5.659
0.9	1.265	0.020－0.145	0.05－0.361	0.248	4.471
1	1.561	0.025－0.149	0.05－0.3	0.201	3.622

In Table 3, T is the wave period, L is the wave length, H is the wave height, k is wave number, A is the wave amplitude ($A=H/2$ for linear regular wave), R is the radius of the cylinder, $R=D/2$, d is depth of water, kA is the wave steepness, kR is the scatter parameter, kd is the water depth parameter. The condition whether a wave belong to deep-water wave is $d/L>0.5$. Since $d/L>0.5$ for all cases satisfying criteria of deep water waves, the regular wave series considered in the present experiment are all deep-water waves.

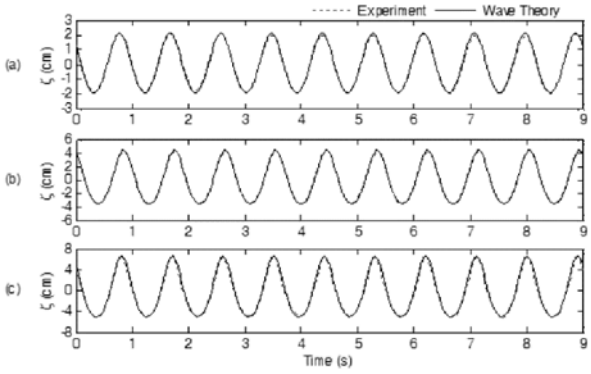

Fig. 2　Comparison between experiments and wave theory. The wave period T=0.9 s, (a) kA=0.1, (b) kA=0.2 (c) kA =0.3.

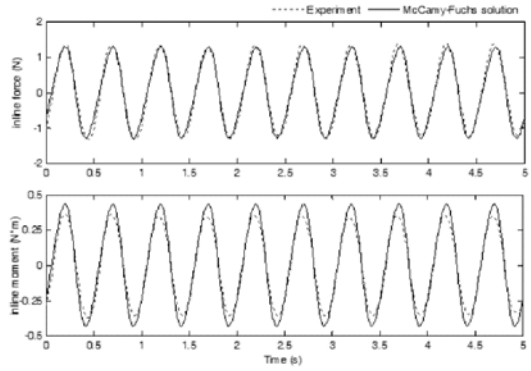

Fig. 3　Comparison between experimental results and McCamy-Fuchs solution. The waves has period T=0.5s, kA =0.2 and kR=0.805.

4　Experimental results at h_s/D=2

4.1 Wave run-up around the vertical cylinder

4.1.1 Running-up wave surface elevation at the front point

The physical process of wave run-up can be described that the kinetic energy of the wave is converted into potential energy, when the wave ran into the vertical cylinder. In other word, the wave which is blocked would climb along the cylinder. The maximum wave run-up would take place at the front point around the cylinder. A_r is the running-up wave surface elevation.

Fig. 4 presents the normalized amplification, A_r/A, of the incident-wave train at the front of the cylinder as a function of kR and kA. We can observe that the amplification, A_r/A, increases as kA increases for most of wave slopes except some steepest wave. Maybe the reason is that kA is so large that the maximum wave run-up is embodied in the wall of the cylinder instead of in the vicinity where the wave gauge is placed, so the maximum wave run-up can not be measured accurately. It turned out that the effect of wave nonlinearity on the wave run-up history plays an important role in the effect of the wave run-up. Besides, the maximum wave run-up increases as kR increases, so we can infer that the effect of the wave run-up is partly influenced by the scatter parameter. The reason can be well-understood: giving the specific wave steepness $kA = 2\pi A/L$, the smaller kR, the larger the amplitude of the incident wave.

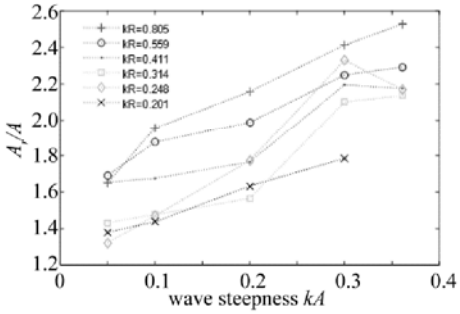

Fig. 4 The normalized surface elevation as a function of wave steepness and scatter parameter

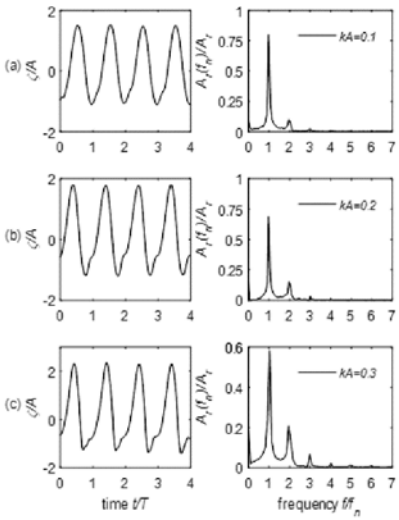

Fig. 5 Time histories of the non-dimensional magnitudes of the free elevation and spectrum analysis with different wave steepness for kR=0.248: (a) kA =0.1; (b) kA =0.2; (c) kA =0.3

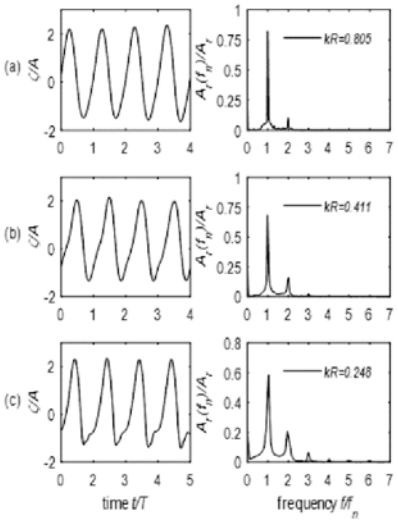

Fig. 6 Time histories of the non-dimensional magnitudes of the free elevation and spectrum analysis with different scatter parameter for kA =0.3: (a) kR=0.805; (b) kR=0.411; (c) kR=0.248

Fig. 5 and Fig. 6 indicate the relation between the normalized surface elevation and wave steepness parameters and scatter parameter, respectively. The normalized maximum run-up increases as *kA* increases, and the shape of the wave crest becomes more and more sharp, the physics of the secondary peak is getting evident, which is due to the superposition effect of different waves, like the incident wave, reflected wave and edge wave. From the spectrum analysis, the non-linear harmonic components increases as *kA* increases or *kR* decreases, which is certified that the number of the significant peak increase from 3 to 5 or 2 to 5.

4.1.2 Running-up wave surface elevation at all points

Though the maximum run-up takes place at the front center of the cylinder, the surface elevation around the cylinder is important for the hydrodynamic property of the artificial structures.

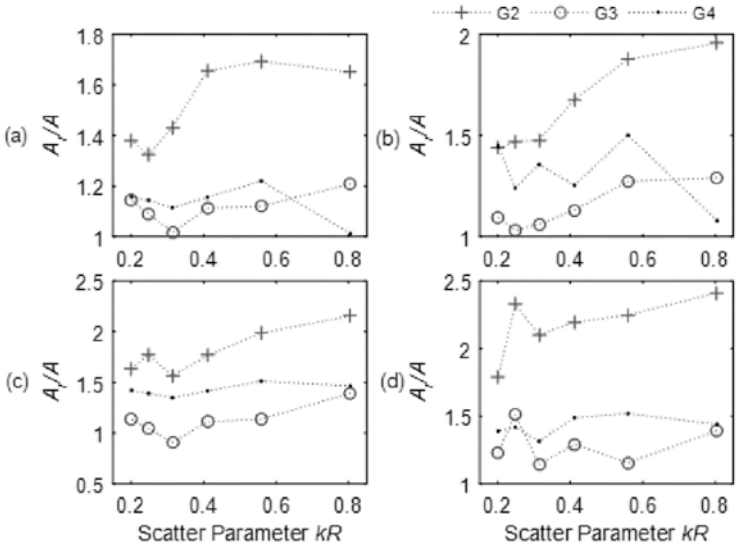

Fig. 7 The non-dimensional magnitudes of the surface elevation as a function of scatter parameter with different wave steepness. (a) *kA*=0.05; (b) *kA* =0.1; (c) *kA* =0.2; (d) *kA* =0.3.

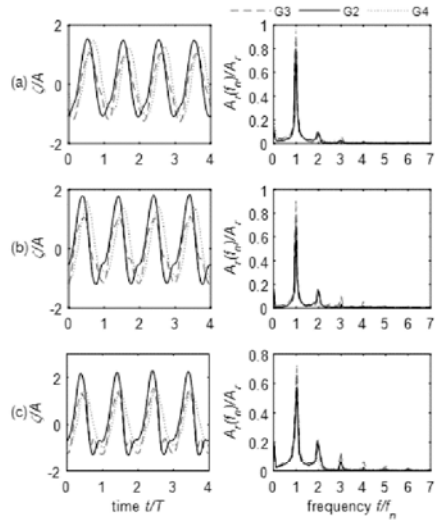

Fig. 8 Time histories of the non-dimensional magnitudes of the free elevation and spectrum analysis at three points around the vertical cylinder with different wave steepness for the specific scatter parameter *kR*=0.248: (a) *kA* =0.1; (b) *kA* =0.2; (c) *kA* =0.3.

Fig. 7 shows the non-dimensional magnitudes of the surface elevation as a function of scatter parameter with different wave steepness. The conclusion that the wave run-up at the front of cylinder was the largest at all positions around cylinder is deduced once more. The maximum wave run-up at the front point (A_r/A(G2)) increases as *kR* increases for most of cases. But for the wave run-up at the rear point (A_r/A(G4)), we can observe that the value is either an approximate constant or fluctuating up and down as *kR* increases. But for the wave run-up at the side point (A_r/A(G3)), the value reaches its minimum in the vicinity of the scatter parameter *kR*=0.3. In most cases, the wave run-up at the rear is larger than that at the side.

Fig. 8 shows the relation between the normalized surface elevation and wave steepness parameters. The conclusion is similar to the one in Section 4.1.1. The wave elevation can indicate that the non-linear harmonic component exists at all three points. The high-order components of the wave run-up at the rear point (G4) is smaller than the others (G2 and G3). The second-order and above components of the wave run-up at the side (G3) is the largest.

4.2 Wave force around the vertical cylinder at $\boldsymbol{h_s/D}$=2

The relation between the inline force and the wave parameters is shown by McCamy-Fuchs solutions, see Section 3.2. If the free-surface elevation is not taken into account, we can compute the integral for $f_x(z,t)$ with the range from $-h_s$ to zero, and an estimation of total inline wave force on a truncated cylinder is calculated as:

$$F_x(t) = \int_{-h_s}^{0} f_x(z,t)\,\mathrm{d}z = \frac{2\rho g H}{k^2} A(kR)\left[\frac{\sinh k(h_s-d)}{\cosh kd} + \tanh(kd)\right]\cos(\omega t - \sigma) \qquad (6)$$

The amplitude of the inline force is nondimensionalized with $\rho g H D d[\tanh(kd)/kd]$

$$F_T{}' = \frac{F_T}{\rho g H D d[\frac{\tanh(kd)}{kd}]} \qquad (7)$$

where F_T is the amplitude of the inline force.

Fig. 9 shows the $F_T{}'$ results obtained by experiments and McCamy-Fuchs solution. It is observed that the experimental results are slightly larger than the McCamy-Fuchs solution. This is possibly due to the higher-order components of the wave for experimental results, while the McCamy-Fuchs solution is only consist of the first order component. While *kR* is smaller than 0.5, $F_T{}'$ results are approximate for different water steepness parameters. It can be concluded that the water steepness parameter is not a significant factor when *kR* is small. However, when *kR* is above 0.6, the difference for different water steepness parameters become more significant. This range represents the high-frequency of the wave measurements, as the high-frequency incident waves are significantly distorted by the scatted waves from the

cylinders.

In the case of regular waves on a flat sea bed, the hydrodynamic forcing on a smooth truncated circular cylinder can be considered a function of the following dimensional parameters:

$$\rho,\ g,\ H, h_s,\ d,\ L,\ R,\ v,\ t$$

where t is time, and v is kinematic viscosity. By dimensional analysis, the inline force can therefore be written as a function of six dimensionless parameter: what we research is different submergence depths, h_s/D is taking into account.

$$\frac{F_x}{\rho g h_s R^2} = f(H/L, d/L, R/L, \frac{h_s}{R}, \frac{v}{\sqrt{gL^3}}, \frac{t}{\sqrt{gL}}) \tag{8}$$

Further, without loss of generality, $v/\sqrt{gL^3}$ can be replaced by Reynolds number, which could be defined in terms of the maximum horizontal velocity at still water $Re = u|_{z=0}D/v$. $F_T$is the amplitude of inline force which is independent of time. Hence, by introducing the wavenumber $k = 2\pi/L$, $R=D/2$, the functional relation for F_T during a wave period can be written

$$\frac{F_T}{\rho g h_s D^2} = f(kA, kd, kR, \frac{h_s}{D}, Re) \tag{9}$$

Besides, the buoyancy force of the semi-submerged vertical circular cylinder in still water can be expressed as:

$$F_{\text{buo}} = \rho g V_s = \frac{\pi}{4}\rho g h_s D^2 \tag{10}$$

So the relation between the inline force and the buoyancy force can be expressed as:

$$\frac{F_T}{F_{\text{buo}}} = f(kA, kd, kR, \frac{h_s}{D}, Re) \tag{11}$$

where $kd \geqslant 1$, we present that all waves are deep-water wave. The difference of kd can be neglected.

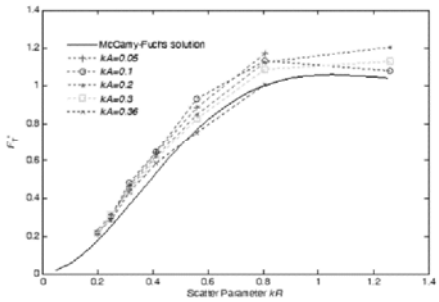

Fig. 9 Comparison between experimental results and McCamy-Fuchs solution. The amplitude of the incline force as a function of wave steepness and scatter parameter.

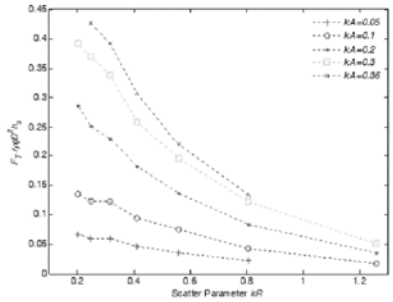

Fig. 10 The normalized inline force at different wave steepness and scatter parameters.

Fig. 10 indicates the relation between the normalized inline force and wave parameters. For the specific wave steepness, the normalized inline force decreases as kR increases. The large scatter parameter means the small wave amplitude when the diameter is constant, and the small wave mainly acts on the cylinder near the free-elevation. The inline force per unit submergence depth decreases as the submergence depth increases. But for the specific scatter parameter, the normalized inline force on the cylinder increases as kA increases, certainly because of the larger wave amplitude.

5 Experiment results with five different submergence depths

5.1 Wave run-up around the vertical cylinder

5.1.1 Running-up wave surface elevation at the front point

Nidzwecki researched the wave run-up at front of full-length and truncated cylinder and concluded that there are no significant differences for the wave run-up on the truncated and full-length cylinders. But the non-linear harmonic components can not be embodies by the amplification of the wave run-up.

Fig. 11 shows the time histories of the non-dimensional magnitudes of the free elevation and spectrum analysis for the specific scatter parameter with different wave steepness and different submergence depths. The time histories of the free elevation are similar and the amplifications of the wave run-up are almost equal for different submergence depths. From the spectrum analysis, the non-linear harmonic components are the same.

5.1.2 Running-up wave surface elevation at the all point

Fig. 12 shows the time histories of the non-dimensional magnitudes of the free elevation and spectrum analysis with kA=0.3 and kR=0.248 with different submergence depths at three positions around the cylinder. The differences at G3 is larger than those at G2 and G4 with different submergence depths, particularly the peak and secondary peak, so that the spectrum analysis make a difference. The secondary peak is due to the superposition effect of the different waves, like the incident wave, reflected wave, and edge wave. The edge wave may be influenced by the submergence depths.

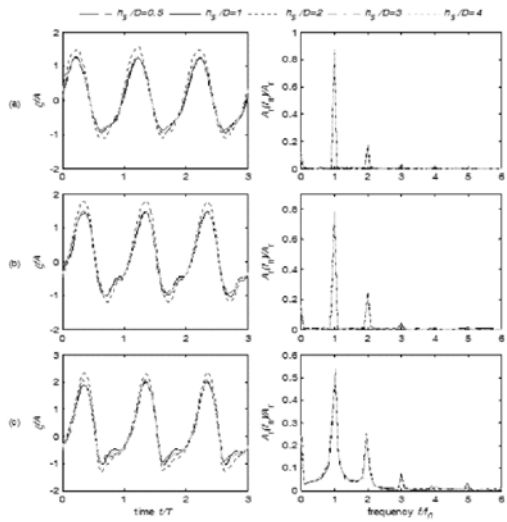

Fig. 11 Time histories of the non-dimensional magnitudes of the free elevation and spectrum analysis with different wave steepness for the specific scatter parameter kR=0.248: (a) kA=0.1; (b) kA =0.2; (c) kA=0.3.

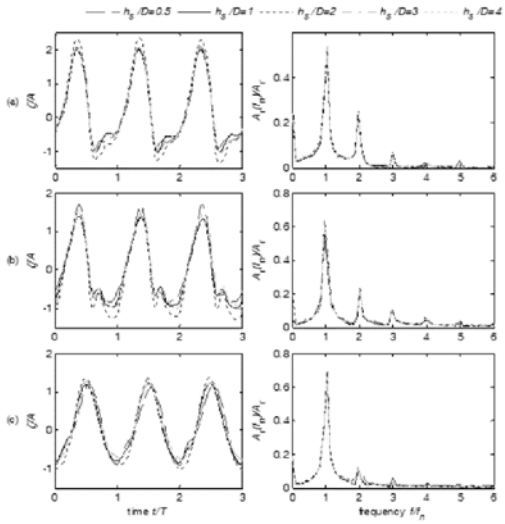

Fig. 12 Time histories of the non-dimensional magnitudes of the free elevation and spectrum analysis with the specific wave steepness kA=0.3 and the specific scatter parameter kR=0.248: (a) G2; (b) G3; (c) G4.

5.2 Inline force dependence on submergence depths

Many artificial structures are vertical cylindrical structures, but some of them are not bottom-mounted like wind turbine foundations. This means the submergence depth may influence the inline force, just as McCamy-Fuchs solution.

Fig. 13 shows the non-dimensional magnitudes of the inline force as a function of wave steepness and submergence depth. It should be noted that when the amplitude of the incident wave is larger than the minimum submergence depth h_s=5 cm, the bottom of the cylinder would be out of the water (OFW). Though the period is short, the slamming loads may be included in the measurements for the inline force. There are four cases which contain the wave impact in the submergence depth h_s=5 cm.

It is observed in Fig. 13 that the non-dimensional magnitudes of the inline force decreases as the submergence depth increases for most of wave slopes, especially for all cases at kR=0.805. It is concluded that the wave force mainly acts water surface. It's well-understood that the wave amplitude has an exponential decay as wave depth increases for the deep-water wave. In Fig. 13a, the large scatter parameter means the small wave amplitude when the diameter is constant, and the small wave mainly acts on the cylinder near the free-elevation. The inline force per unit submergence depth decreases as the submergence depth increases. Beside, for each submergence depth, the inline force increases as kA increases for all the cases, certainly because of the larger wave amplitude. But in Fig.13b-d, the non-dimensional magnitudes of the inline force as $h_s/D = 0.5$ is close to the value as $h_s/D = 1$. In other words, while h_s/D is between 0.5 and 1, the ratio of the inline force to buoyancy force is approximate constant for some kR, then the ratio decreases as the submergence depth increases.

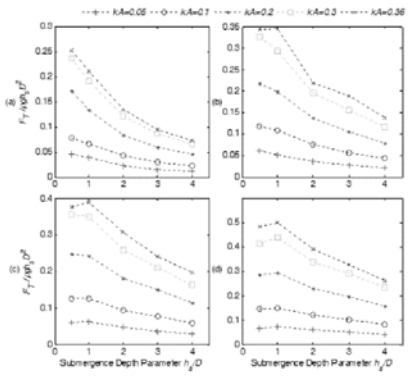

Fig. 13 The non-dimensional inline force as a function of wave steepness and submergence depth. (a) T=0.5 s, kR =0.805; (b) T=0.6 s, kR =0.559; (c) T=0.7 s, kR =0.411; (d) T=0.8 s, kR =0.314.

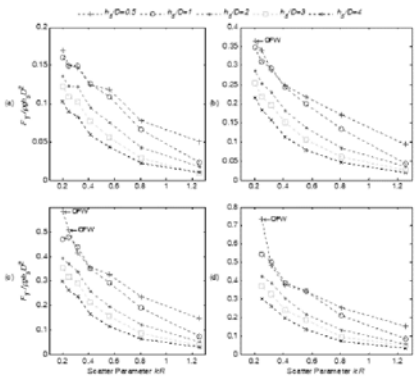

Fig. 14 The non-dimensional inline force as a function of scatter parameter and submergence depth. The case with out of water (OFW) have been marked with the arrow (a) kA =0.1; (b) kA =0.2; (c) kA =0.3; (d) kA =0.361.

Fig. 14 shows the relation between the scatter parameter, submergence depth and the non-dimensional magnitudes of the inline force. It is observed that the non-dimensional magnitudes of the inline force decreases as kR increases for most cases. It should be noted that the range of $0.2<kR<0.6$, the ratio of the inline force to buoyancy force is approximately constant, excepting the cases that the bottom of the cylinder is out of water (see the arrowhead crosswise dot in Fig. 14).

6 Conclusions

We have performed an extensive set of experiments for a semi-submerged vertical circular cylinder with different submergence depths in regular waves. The purpose is to measure the wave run-up and horizontal wave loads acting on the cylinders. The non-dimensional magnitudes of the wave run-up and inline force are both measured on the cylinder with different submergence depths.

For each cylinder, the results clearly showed that the non-dimensional magnitudes of the inline force decreases when the incident-wave steepness decreases or scatter parameter increases. It also showed increases in the normalized maximum run-up when the incident-wave steepness were increases or scatter parameter increases, and the shape of the wave crest becomes more and more sharp. From the spectrum analysis, the non-linear harmonic components increase as the kR decreases or kA increases.

Based on the experimental results, it is concluded that the wave forces are clearly influenced by the submergence depths. The results clearly showed that the non-dimensional magnitudes of the inline force decreases when the submergence depths or kR increases. The condition is that the ratio of the inline force to buoyancy force is approximately constant while h_s/D is between 0.5 and 1 and kR is between 0.2 and 0.6. No significant differences for the wave run-up on the truncated cylinder with different submergence depths is observed. The differences of the non-linear harmonic components at G3 is quite influenced by the submergence depths.

Acknowlegdement- The authors would like to thank Mr. Rong Huixiang, Mr. Deng Yanfei and Mr. Guan Lei for their assistance on the test installations.

References

1 Morison J R, O'Brien M P, Johnson J W and Schaaf S A. The forces exerted by surface waves on piles[J]. J. Petrol. Tech., 1950.2 (5): 149–154.
2 Mccamy, R. and Fuchs, R. Wave Forces on Piles: A Diffraction Theory[R]. Tech. Memo No. 69, Beach Erosion Board, U.S. Army Corps of Engineers, Washington D. C, USA. 1954.
3 Oguz Yilmaz and Atilla Incecik. Analytical solution of the diffraction problem of a group of truncated vertical cylinders[J]. Ocean Engineer, 1998,25(6):385–394.
4 Galvin C J, Hallermeier R J. Wave run-up on vertical cylinders[C]//Proc.13th Intl. Conf. on Coastal Engineering, Vancouver, Canada, 1972:1955–1974.
5 Huseby M and Grue J. An experimental investigation of higher-harmonic wave forces on a vertical cylinder[J]. J. Fluid Mech., 2000,414, 75–103.